JOURNAL OF Materials CHEMISTRY

Metal citrate polymerized complex thermal decomposition leading to the synthesis of $BaTiO_3$: effects of the precursor structure on the $BaTiO_3$ formation mechanism

Pedro Durán,[a] Francisco Capel,[a] Dionisio Gutierrez,[a] Jesús Tartaj,[a] Miguel A. Bañares[b] and Carlos Moure[a]

[a]*Instituto de Cerámica y Vidrio (CSIC), Electroceramics Department, 28500 Arganda del Rey, Madrid, Spain*
[b]*Instituto de Catálisis y Petroleoquímica (CSIC), Campus UAM, Cantoblanco, 28049 Madrid, Spain*

Received 19th December 2000, Accepted 27th April 2001
First published as an Advance Article on the web 5th June 2001

The study of $BaTiO_3$ crystallization from X-ray amorphous (Ba,Ti) polymeric organic powders has been carried out by comparing samples previously heat-treated in air at 250 and 400 °C. From thermal analysis, X-ray diffraction, infrared and Raman spectroscopies, and ^{13}C NMR spectroscopy, it has been found that the $BaTiO_3$ formation strongly depends upon the initial structure of the used precursor. It is concluded that an intermediate oxycarbonate phase was formed prior to the formation of $BaTiO_3$ above 550 °C when the precursor used was a (Ba,Ti)-mixed metal organic complex heat-treated at 250 °C, and a nanocrystalline $BaCO_3$ intermediate when the metal organic complex had been initially heat-treated at 400 °C. Although not well crystallized, thermoanalytical measurements, the unique XRD pattern, and new IR and Raman structural features revealed that such a metastable intermediate oxycarbonate phase has a stoichiometry close to $Ba_2Ti_2O_5{\cdot}CO_3$, which is characterized by having CO_3^{2-} groups different to those of pure $BaCO_3$ located, probably, in an open interlayer $BaTiO_3$ metastable structure. Irrespective of the used precursor, thermal decomposition of the (Ba,Ti)-mixed metal organic above 550 °C led to the formation of a mixture of tetragonal and hexagonal $BaTiO_3$ polymorphs rather than cubic. The synthesized $BaTiO_3$ powders are characterized by a high surface area of 40 $m^2\ g^{-1}$ up to 700 °C, and an equivalent particle size smaller than 25 nm. Raman spectra indicated asymmetry inside the TiO_6 octahedra of the $BaTiO_3$ structure.

Introduction

Although a number of investigations have contributed to a better knowledge of the reactions involved in the thermal decomposition synthesis of $BaTiO_3$,[1–6] there have been four major efforts over the last 25 years to establish as unambiguously as possible the reaction mechanism(s) taking place during the thermal decomposition of the (Ba,Ti) organic precursors for $BaTiO_3$ formation.[7–10]

Gopalakrishnamurthy *et al.*[7] were the first to report the existence of an oxycarbonate-like intermediate phase ($Ba_2Ti_2O_5{\cdot}CO_3$) as the key for the formation of $BaTiO_3$ during the thermolysis of barium titanic oxalate in air. Hennings and Mayr[8] studied the thermal decomposition of (Ba,Ti) citrate salts and assuming a complete molecular-level mixing of barium and titanium cations, concluded that prior to the formation of $BaTiO_3$ an intermediate with the overall composition $BaCO_3{\cdot}TiO_2$ was formed. In both cases the conclusions were based on the obtained experimental results using classical techniques such as XRD, TG/DTA, and IR. Albeit with some discrepancy on the types of intermediate phases involved, it was generally accepted that the formation of $BaTiO_3$ from the thermal decomposition of organic precursors involves the following three main steps as the calcination temperature was increased: (i) dehydration reaction, (ii) decomposition/oxidation reactions of the organic species to form intermediate phases such as $BaCO_3{\cdot}TiO_2$, $BaCO_3{\cdot}TiO_2$ and $Ba_2Ti_2O_5{\cdot}CO_3$, and (iii) reaction between the formed intermediate phases or the decomposition of the metastable $Ba_2Ti_2O_5{\cdot}CO_3$ phase leading to the formation of $BaTiO_3$ as the final reaction product.

Kumar *et al.*[9] on the basis of XRD, TG/DTA, and Raman spectrometry data, found that an oxycarbonate intermediate phase, and not a mixture of $BaCO_3$ and TiO_2, as proposed by Henning and Mayr,[8] forms in the thermal decomposition of (Ba,Ti)–citrate based organic precursors previously heat-treated at 375 °C for 10 h. The stoichiometry of such an intermediate phase was considered to be close to $Ba_2TiO_2O_5{\cdot}CO_3$, and the $BaTiO_3$ was formed from the endothermic decomposition of the intermediate phase in the temperature interval 635–700 °C.

Recently, Durán *et al.*[10] reported, although not conclusively, that depending on the heating rate, the $BaTiO_3$ formation could take place *via* a predominant solid-state reaction between nanosized $BaCO_3$ particles and amorphous $TiO_2(TiO_{2-x})$ when crystallised using a low heating rate (<1.5 °C min^{-1}), although a relatively small amount of a quasi-amorphous oxycarbonate intermediate phase was also present. $BaTiO_3$ crystallization using a rapid heating rate ($\geqslant 5$ °C min^{-1}) took place through formation of a quasi-amorphous oxycarbonate phase, as the main rate-controlling factor for the crystallisation process. The formation of oxygen-deficient hexagonal $BaTiO_3$ coexisting with the tetragonal $BaTiO_3$ polymorph up to 700 °C also was suggested.

In all the above a common fact, the formation of an oxycarbonate phase alone or accompanied by other by-products, was reported as the controlling-rate factor for the $BaTiO_3$ formation. More recently, Gablenz *et al.*[11] have shown additional evidence for the existence of such an oxycarbonate intermediate phase based on electron energy loss spectroscopy (EELS) measurements, and quantum-mechanical calculations using density functional theory (DFT). However its formation,

 DOI: 10.1039/b010172i

nature, stability, and the role played during the synthesis of $BaTiO_3$, have not unambiguously clarified and in some cases questioned.[12,13]

Based on our previous studies,[10] we believe that the mechanism of the $BaTiO_3$ synthesis can change not only with the heating rate regime but also with the previous thermal history of the polymeric precursors. In the present paper the thermal behaviour of two polymeric precursors previously heat-treated at two different temperatures is studied. An attempt to synthesize the oxycarbonate intermediate phase from (Ba,Ti)–citrate polymerised amorphous precursors, is undertaken, and its chacterization using TG/DTA, XRD, IR, and ^{13}C NMR techniques made. Its stability and thermal evolution, leading to $BaTiO_3$ formation, is also studied using XRD, IR and room temperature Raman spectroscopies.

Experimental procedure

(1) Preparation of the powder precursors

Barium nitrate $Ba(NO_3)_2$ (99.99%, Aldrich), and titanium tetrabutoxide $Ti(C_4H_9O)_4$ (99.9%, Alfa Aesar), were the precursors used for $BaTiO_3$. A slightly acid ethylene glycol (EG) solution of titanium tetrabutoxide was mixed with an aqueous citric acid (CA) solution by stirring and heated at 60 °C for 2 h. The clear obtained solution was then mixed with an aqueous barium nitrate solution such that the barium and titanium were equimolar. A molar ratio of Ba : Ti : CA : EG = 0.1 : 0.1 : 1 : 4 was used. This mixed solution was heated to 80 °C for 2 h. A transparent solution was obtained indicating that the mixing of barium and titanium cations was on the molecular level. In order to promote the esterification reaction the above clear solution was heated to 130 °C for 2 h. A change to pale yellow took place and then the solution was concentrated by heating to 180 °C for 3 h. The solution became more viscous and turned brown. No visible precipitation was observed during this heating process. Finally the viscous solution was heated to 250 °C for several hours, and a solidified dark brown spongy resin, hereinafter referred to as the ''polyester resin'' or PR powder, was obtained. In order to minimize the strong exothermicity of the thermal decomposition process, the resin was converted into a powder by grinding with a Teflon bar, and then calcined at a heating rate of 2 °C min^{-1} at 400 °C for 4 h in air. This powder will be hereinafter referred to as the ''prepyrolyzed precursor'' or PP powder. All further thermal analyses were performed on these two precursor powders.

(2) Powder characterisation

The thermal analyses were carried out with a thermoanalyser (STA 409, Netzsch–Geratebau, Selb–Bayern, Germany) which records DTA and TG simultaneously. 150 mg samples were placed in platinum crucibles, using calcined alumina as a reference material. The heating rate was 10 °C min^{-1} and the thermal analyses were carried out in flowing air. The resultant phases in both the ''polyester resin'' and the ''pre-pyrolyzed precursor'' heat-treated in the temperature range 400–750 °C, were identified by CuKα X-ray diffraction (XRD), 50 kV–30 mA (Siemens D-5000, Erlangen, Germany). The scan rate was 2° min^{-1} for phase identification in the 2θ range 2–75° and step scanning (step size 0.002, counting time 10° $step^{-1}$) was used for the determination of the lattice parameters, where standard silicon powder was used for the angle calibration. Crystallite sizes of calcined powders were determined by X-ray line broadening using the Scherrer equation.[14] The specific surface areas of the calcined powders were measured with nitrogen by single-point BET (Quantachrome MS-16 model, Syosset, NY). IR spectra were recorded with a FT-IR spectrometer (Perkin Elmer 1760 X, Beaconsfield, England) in the range 400–4000 cm^{-1} on as-pressed disks using KBr as the binding material. IR spectra were used to characterize the ligand coordination made in the heat-treated (Ba,Ti)-polymeric precursors.

The molecular structure and cation coordination of the two types of calcined powder precursors was studied using Raman spectroscopy. Raman spectra were registered at room temperature with a single monochromatic Renishaw system 1000 equipped with a cooled CCD detector (−73 °C) and a holographic Notch filter. The elastic scattering was filtered by a holographic Notch filter, and the Raman signal remained higher than with triple monochromatic spectrometers. The samples were excited with the 514 nm Ar line during *in situ* treatments. The resolution was better than 2 cm^{-1}, and the spectra acquisition consisted of five accumulations of 60 s. The powder morphology was examined by scanning electron microscopy (SEM) (Zeiss DSM 950, Oberkochem, Germany).

The high-resolution solid-state ^{13}C NMR spectra were obtained at room temperature on a Bruker MSL 400 spectrometer at a frequency of 100.63 MHz for ^{13}C. The standard CPMAS pulse sequence was applied with a 6.5 μs ^1H-90° pulse width, 3 ms contact pulses and 5 s repetition time. In the case $BaCO_3$ a single pulse sequence was applied with 6 μs 90° pulses and 30 s repetition time. The spinning frecuencies were, in all cases, 4 kHz. The number of scans varied between 800 and 1600. All chemical shifts (δ) are given with respect to the TMS signal.

Experimental results

(1) Powder precursor characterisation

Fig. 1 shows SEM micrographs of the two PR and PP powder precursors heat-treated at 250 and 400 °C, respectively. As can be observed, the PR powder was revealed to have a friable and spongy aspect while the PP powder was an agglomerated powder with agglomerate sizes of about 200 nm. Fig. 2 shows the XRD patterns of these two kinds of precursors. In both cases the amorphous character of the powders is preserved at this thermal level while strong exothermal combustion of the resin in the prepyrolyzed precursor could destroy its local structure. In fact, the PP powder after several days exposed to ambient air showed the presence of crystalline $BaCO_3$ by XRD measurements. Then the study of the thermal decomposition behavior of this precursor was carried out on fresh PP powders. The FT-IR spectra of both powder precursors are shown in Fig. 3. Although the IR spectrum of the PR powders was very complex, the presence of broad bands at 3445 cm^{-1} (water stretching vibrations),[15,16] 2961 cm^{-1} (C–H stretching modes),[17] 1736 cm^{-1} (C=O stretching modes for the ester group),[6] 1625 and 1569 cm^{-1} (antisymmetric COO stretching mode for a unidentate complex and a bridging complex, respectively),[18] 1389 cm^{-1} (stretching vibrations of a unidentate complex), were evident.[19] These, along with broad bands at 1450, 1043, 860, and 622 cm^{-1} (assigned to carbonate ions)[8] and, finally, broad bands at 776 and 545 cm^{-1} (Ti–O stretching modes), characterised a relatively well dehydrated PR precursor.

The IR spectrum of the PP powder showed several significant changes with respect to that of the PR powder (see Fig. 3). First, the appearance of a sharp peak at 2340 cm^{-1} relates to CO_2 adsorbed on a metal cation (gaseous CO_2 gives a band at 2360 cm^{-1}). Second, all the IR broad bands narrowed and decreased in intensity. Third, a new peak at 1410 cm^{-1} which can be attributed to residual carboxylate ions,[6] and the peaks at 1450, 1059, 857, and 670 cm^{-1} assigned to carbonate ions were better developed; and fourth, the two peaks at about 800 and 534 cm^{-1} for Ti–O stretching in TiO_2 (anatase), were clearly detected. All these changes in the IR spectrum can be interpreted as a global evolution from unidentate and bridging carboxylate complexes to bidentate ones with the formation of metal cation–carboxylate group ionic bonds.

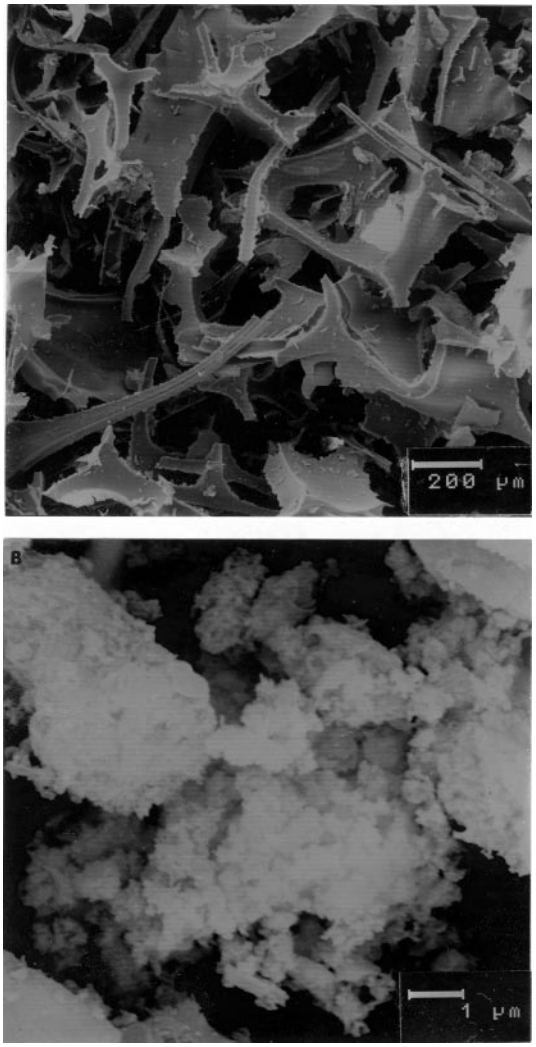

Fig. 1 SEM micrographs of the PR precursor and PP powder.

The solid-state ^{13}C NMR spectra of PR and PP powder precursors are shown in Fig. 4. In both samples ^{13}C resonance absorptions for the carboxyl groups, terminal –COOH, at about 174 and 187 ppm, and internal COOH at about 178 and 190 ppm, respectively, were present. A strong resonance signal at about 131.7 ppm may be due to unsaturated carbon (C=C) produced in the dehydration of the PR powder. Two resonance signals at about 72 and 895 ppm attributable to a central carbon, C(OH), were also observed. The presence of other

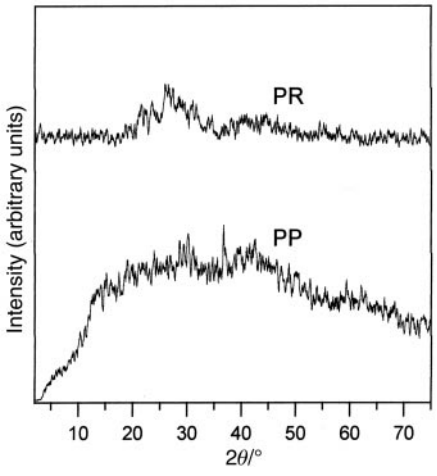

Fig. 2 XRD patterns of polyester resin and prepyrolysed precursor powders.

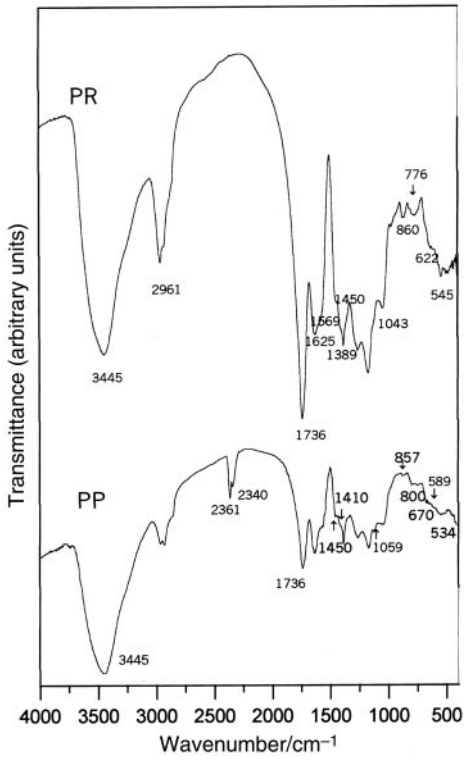

Fig. 3 FT-IR spectra of PR and PP powders.

functional groups such as $–CH_2–$, which are not involved in the complexation process, were detected mainly by the resonance signal at 43 ppm.[20]

Two relevant differences between the spectra are seen to occur: (i) the intensity of resonance signals was strongly decreased for the PP powder, and (ii) an additional resonance signal, which can be attributed to the carbonate group (CO_3^{2-}), appeared at about 1675 ppm in the ^{13}C NMR spectrum of the PP powder. A comparison between the two ^{13}C NMR spectra suggests that the structure of the (Ba,Ti)–citrate organic complex powder essentially collapses when it is prepyrolyzed at 400 °C.

(2) Thermal decomposition behaviour of the powder precursors and characterization

Fig. 5 shows the TG/DTA curves at a heating rate of 10 °C min^{-1} in flowing air for PR and PP powders between room temperature and 900 °C. The thermal decomposition of the PR precursor exhibited a multistep exothermal process

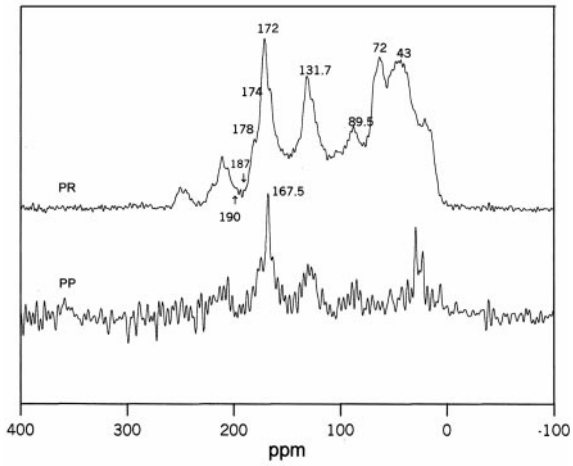

Fig. 4 Solid-state ^{13}C NMR spectra of PR and PP powders.

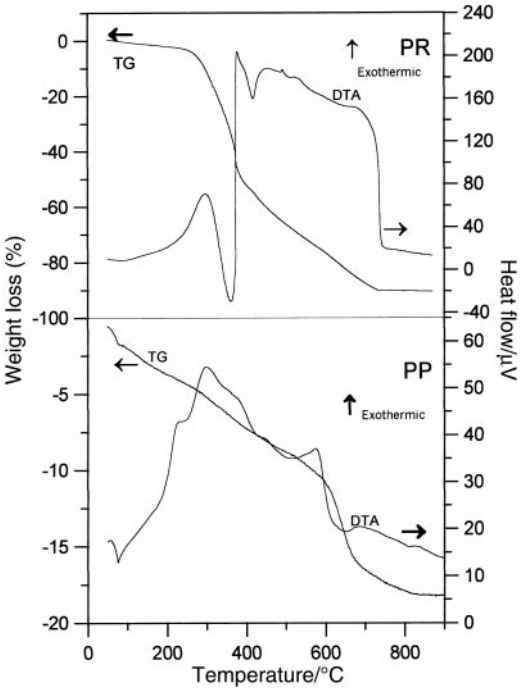

Fig. 5 TG and DTA of PR powder and PP powder.

which is completed at about 740 °C. According to the TG curve, the thermal decomposition process is characterized by three apparent decreases in sample weight over the temperature ranges 200–360 °C, 370–430 °C, and 430–730 °C. Each of the decreases in the TG curve corresponds to an exothermic peak in the DTA curve. No endothermic effects were detected in the DTA curve. As previously reported elsewhere,[10] given that no weight gain was registered during the thermal decomposition of the PR precursor, we have to assume also now that the main reactions occurring with increasing temperature in the formation of $BaTiO_3$ from (Ba,Ti)–citrate polyester resin precursors, are the following: (a) dehydration of the PR precursors, (b) decomposition/oxidation of the dehydrated PR precursor with the formation of the intermediate phases, and (c) formation of barium titanate as a consequence of the reaction between the previously formed intermediate by-products.

The thermal decomposition of PP precursors under the same experimental conditions as for the PR sample shows the following features: below 600 °C the thermal decomposition process shows similar exothermic effects as for the PR precursor, in which residual hydration water and organic compounds are eliminated. The only differences are the presence of two relatively small endothermic peaks at about 640 and 820 °C, which may correspond to the decomposition of an oxycarbonate intermediate phase and to residual $BaCO_3$, respectively. Furthermore, the total weight loss was about 18%, which is in close agreement with the theoretical loss (16%) for the formation of $BaTiO_3$ *via* a solid-state reaction between nanocrystalline $BaCO_3$ and amorphous TiO_2, in agreement with the suggestions of Hennings and Mayr.[8]

Fig. 6 shows the FTIR spectra for precursors PR and PP calcined at different temperatures. The IR spectra of the PR powder showed bands at 3435, 2960, and 1760 cm^{-1} corresponding to the O–H, C–H and C=O stretching modes, respectively, which were similar to those of the PP precursors calcined at 400 °C, but the relative intensities at 1625 and 1569 cm^{-1} related to the antisymmetric COO stretching mode of unidentate and bridging complexes, respectively, are much stronger. When calcined at 500 °C for 2 h, the peaks corresponding to the CO_3^{2-} group at about 1436, 1059, 856, and 693 cm^{-1}, and the shoulder at 1410 cm^{-1} corresponding to the carboxylate ions, are all similar to those present for the precursor PP calcined at this same temperature (see below). A broad band at about 574 cm^{-1}, which is typical of the Ti–O vibrations in $BaTiO_3$ also starts to develop. At this calcination temperature there are two additional peaks at about 675 and 874 cm^{-1}, which could not be assigned to any bands of the barium oxide–titanium oxide system and they had not been previously reported in the literature. A similar IR spectrum was observed when the PR precursor was calcined at 550 °C, although the peak at 674 cm^{-1} disappeared and that at

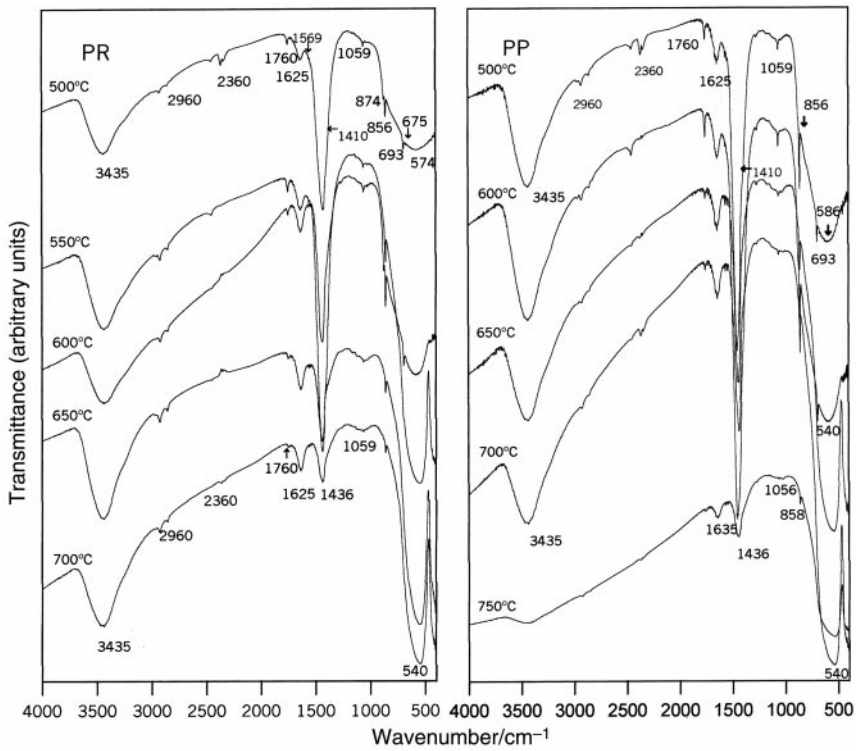

Fig. 6 FT-IR spectra of PR and PP powders heat-treated at the indicated temperatures.

874 cm^{-1} decreased in intensity. It should be mentioned here that the peaks at 1435, 1059, 856, and 693 cm^{-1}, which are characteristic of the CO_3^{2-} group, were always broader than those assigned for the same CO_3^{2-} group in the PP precursor calcined at these two temperatures. These new IR structural features coincided, as we will see later, with the fact that at this temperature interval, *i.e.*, between 500 and 550 °C, the major phase detected by XRD was the intermediate oxycarbonate. With increasing calcination temperature above 550 °C, the extra IR peaks disappeared while the other IR bands decreased in intensity and almost disappeared at 700 °C. Simultaneously, the band corresponding to the Ti–O vibrations in $BaTiO_3$ was better developed and evolved, giving a constant frequency value of 540 cm^{-1}.

As is also shown in Fig. 6, above 400 °C the intensities of the absorption bands at about 3435, 2960, 1760 and 1410 cm^{-1} decreased, and the bands at about 1436, 1059, 856, and 693 cm^{-1} which are characteristic of a carbonate phase,[8] narrowed and increased in intensity for the PP precursor. With increasing calcination temperature the intensity of all of these bands decreased and almost disappeared near 750 °C. Simultaneously, an IR absorption band at about 540 cm^{-1}, which is characteristic of the Ti–O vibrations modes in $BaTiO_3$, became clearer.

The phase development with increasing calcination temperature, in both the PR and PP powders, was also studied by XRD and Raman spectroscopy on calcined samples in the temperature range 500–750 °C at a heating rate of 10 °C min^{-1}. Fig. 7 shows the XRD patterns for PR and PP powders. As previously shown, the PR powder fired at 250 °C was amorphous in structure, and a broad continuum in the XRD patterns was also present after calcining up to 400 °C for 2 h.

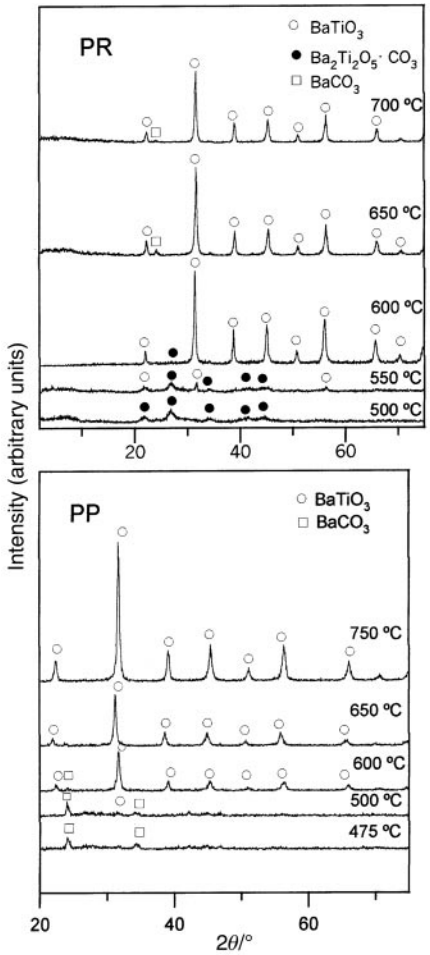

Fig. 7 XRD patterns showing the phase evolution with calcination temperature of PR and PP powders.

Above that temperature and up to 550 °C only broad diffraction reflections which could be clearly identified as to correspond mainly to the so-called intermediate oxycarbonate phase ($Ba_2Ti_2O_5{\cdot}CO_3$) claimed by Kumar *et al.*[9] and corroborated by Arima *et al.*,[21] although some of these diffraction peaks can also be attributable to residual $BaCO_3$, to an oxygen-deficient TiO_{2-x} or to an incipient hexagonal $BaTiO_3$. Above 550 °C, $BaTiO_3$ began to be formed and the oxycarbonate phase slowly decreased and almost disappeared at about 600 °C. Simultaneously to the disappearance of the oxycarbonate intermediate phase, $BaCO_3$ was formed and also disappeared above 700 °C.

The XRD patterns showed that, for PP precursors, $BaCO_3$ was the predominant crystalline phase already from 475 °C, and it was almost the only intermediate phase involved during the transformation of the PP precursor into $BaTiO_3$ with increasing calcination temperature. Such an intermediate phase was not completely eliminated until the temperature was raised up to 750 °C. Contrary to the results of Kumar *et al.*[9] and Arima *et al.*,[21] it is clear the formation of a crystalline $BaCO_3$ phase occurs during the transformation of PP precursor, and although TiO_2 was not simultaneously detected it can be considered that the precursor structure had been, at least at the local level, collapsed and the formed free barium oxide rapidly carbonated.[15,22] This result supported the previous contention of Hennings and Mayr[8] and Vasyl'kiv *et al.*,[12] whose results precluded and even questioned the existence of the so-called oxycarbonate intermediate phase ($Ba_2Ti_2O_5{\cdot}CO_3$).

At this point it should be noted that between 600 and 750 °C a broad peak at about 45.2° was always present in our XRD data and no clear splitting could be detected. XRD patterns for powders heat-treated within this temperature interval were indexed on an *m*3*m* cubic unit cell and a lattice parameter of $a = 0.4041 \pm 0.0005$ nm was measured, which is in close agreement with that of Busca *et al.*[17] ($a = 0.4036$ nm). The particle size of the powders shifted from 15 nm at 600 °C to 30 nm at 750 °C. In this temperature region there are serious line broadening effects due to the small size of the formed $BaTiO_3$ particles, and for this reason it becomes difficult to distinguish between cubic and tetragonal barium titanate phases by means of XRD. Above 900 °C the XRD reflections became sharper and a gradual splitting of the pseudo-cubic [200] into tetragonal [200] and [002] was observed. Then the XRD patterns of the powders were indexed on a 4*mm* tetragonal unit cell. Lattice parameters were measured and a *c*/*a* ratio value close to 1.01 could be calculated, for samples in which a clear splitting was apparent ($\geqslant$1100 °C) (see Fig. 8).

In order to support the above statements, the PR and PP powders calcined in the same temperature range, were

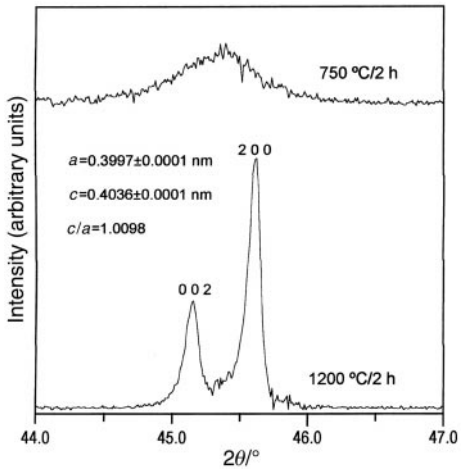

Fig. 8 XRD diffractograms over the 2θ range 44–46° of $BaTiO_3$ after calcination at the indicated temperatures.

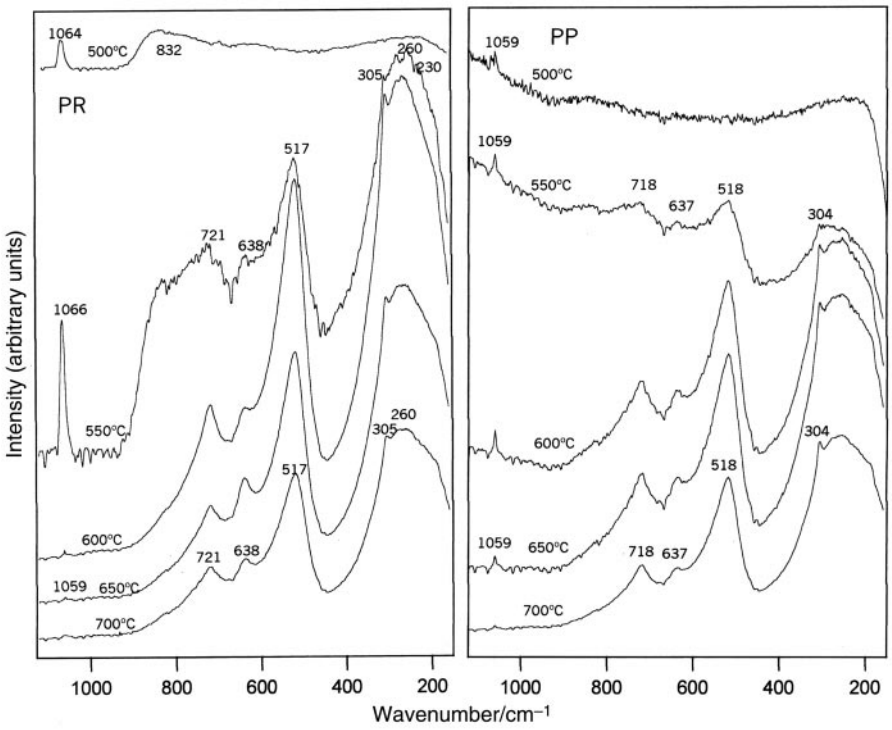

Fig. 9 Raman spectra of PR and PP powder products after heat-treatment at the indicated temperatures.

characterised using room temperature Raman spectroscopy. Fig. 9 shows the Raman spectra for PR and PP powders calcined at 500–700 °C. The Raman spectrum of the PR powder calcined at 500 °C exhibited a fluorescent-like background and only a broad band at 832 cm^{-1} and a sharper band at 1064 cm^{-1} were detected. This last Raman band is characteristic of the CO_3^{2-} symmetric stretching mode. The spectrum of the PR precursor calcined at 550 °C for 2 h showed some new relevant features: (i) the intensity of the peak corresponding to the CO_3^{2-} ions strongly increased, (ii) the peak frequency shifted up to a value of 1066 cm^{-1}, (iii) the appearance of new broad bands at 721, 517, 305 and 260 cm^{-1} which are characteristic of $BaTiO_3$ with tetragonal structure. (iv) A further two new bands at about 638 and 230 cm^{-1} started to develop, which can be attributed to an incipient $BaTiO_3$ with hexagonal structure.[23] With increasing calcination temperature, both the Raman bands for tetragonal and hexagonal $BaTiO_3$ polymorphs increased in intensity up to 650 °C, and the band characteristic of the CO_3^{2-} group, which decreased to 1059 cm^{-1}, almost disappeared. The shift of the carbonate ions peak frequency from about 1066 to 1059 cm^{-1} between 550 and 650 °C, can be related with the formation of some $BaCO_3$ following proposed decomposition of the oxycarbonate intermediate phase, which rapidly reacts with residual titanium oxide above 700 °C. The disappearance of the main carbonate ions peak supported this contention.

As for the PR calcined powders, the spectrum of PP calcined precursors at the lower temperature, *i.e.*, 500 °C, was a broad continuum except for a sharp band at 1059 cm^{-1} indicating the presence of the characteristic CO_3^{2-} peak which, according to the previous XRD results, see Fig. 7, corresponds to crystalline $BaCO_3$ within an amorphous matrix. With increasing temperature, all spectra exhibited the three distinct bands at about 718, 518, and 304 cm^{-1} which correspond to $BaTiO_3$ with tetragonal structure, while the other two bands at about 1059 and 637 cm^{-1} whose intensities increased and decreased, respectively, both disappeared above 700 °C. As mentioned above, the band at 637 cm^{-1} was attributed to the presence of a low temperature stabilised hexagonal $BaTiO_3$ phase. The band at 1059 cm^{-1} is representative of the carbonate phase, and does not shift its frequency with increasing temperature. These results are consistent with the previous assumption that the formation of $BaTiO_3$, for the PP precursor, involves crystalline $BaCO_3$ as the main intermediate phase which reacts with amorphous TiO_2 to form a mixture of hexagonal and tetragonal $BaTiO_3$ polymorphs, and are in good agreement with previously reported results.[8,24] It should be noted here that since Raman spectroscopy is much more sensitive to probe the local rather than long range structure, the presence of a peak at about 305 cm^{-1} in the spectra of both kinds of sample heat-treated at 550 °C indicates, at least on a local scale, asymmetry within the TiO_6 octahedra of the $BaTiO_3$ structure and, contrarily to the XRD results, the as-prepared powders are tetragonal rather than cubic. It could be suggested that the symmetry of the crystals as observed by Raman spectroscopy indicates a local and dynamic symmetry, while the symmetry determined by XRD measurements is an average and static symmetry.

(3) Synthesis, thermal stability and structural features of the intermediate oxycarbonate phase

In order to establish as unambiguously as possible the existence of the "so-called" intermediate oxycarbonate $Ba_2Ti_2O_5{\cdot}CO_3$ phase prior to the $BaTiO_3$ formation, the PR powder was milled for 2 h and sieved below 100 μm. Such a fine PR powder was calcined at a heating rate of 10 °C min^{-1} up to 500 °C and maintaining this temperature for 2 h. To investigate its thermal behaviour, the synthesized oxycarbonate phase was studied by differential thermal analysis and its stability was studied by XRD for isothermally heat-treated samples in the 480–524 °C temperature range for several hours.

Fig. 10 shows the XRD patterns of the synthesized oxycarbonate phase in air for the PR precursor and, for comparison, that corresponding to the PP precursor heat-treated under the same conditions. As is clearly shown, the PP precursor led to the formation of crystalline $BaCO_3$ as the intermediate phase before the formation of $BaTiO_3$, although a negligible amount of the oxycarbonate intermediate phase was also present. In the case of the PR precursor a poorly crystallised phase but clearly different to both $BaCO_3$ or

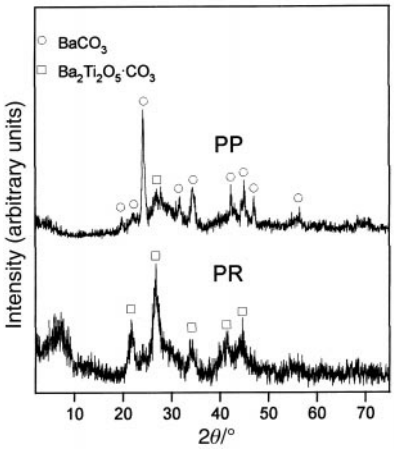

Fig. 10 XRD patterns of PR and PP powders after calcination at 500 °C for 2 h showing the predominance of the oxycarbonate intermediate phase and barium carbonate, respectively.

$BaTiO_3$ was developed. Furthermore, no diffraction peaks corresponding to these last two phases were detected. Therefore, although not well crystallised, the presence of a new phase is clearly evident whose main diffraction peaks were detected at $2\theta = 21.8°$ (56), 24.2° (37), 26.8° (100), 30.2° (32), 32.3° (29), 33.8° (41), 40.8° (40), 44.9° (47), and 54.4 (10%). These diffraction peaks closely coincide with those found for the intermediate oxycarbonate phase claimed by Kumar *et al.*[9] and Arima *et al.*[21] Fig. 11 shows the XRD evolution of the synthesized oxycarbonate intermediate with increasing temperature. As can be observed, the amount of the oxycarbonate phase first slightly increased with both the temperature and the heat-treatment time up to 495 °C, see Fig. 11c, and as soon as the $BaTiO_3$ began to be formed the amount of the oxycarbonate phase slowly decreased and almost disappeared after a heat-treatment for 20 h at 524 °C. From these results it seems clear that the oxycarbonate phase is stable within a relatively wide temperature range, and its transformation is the

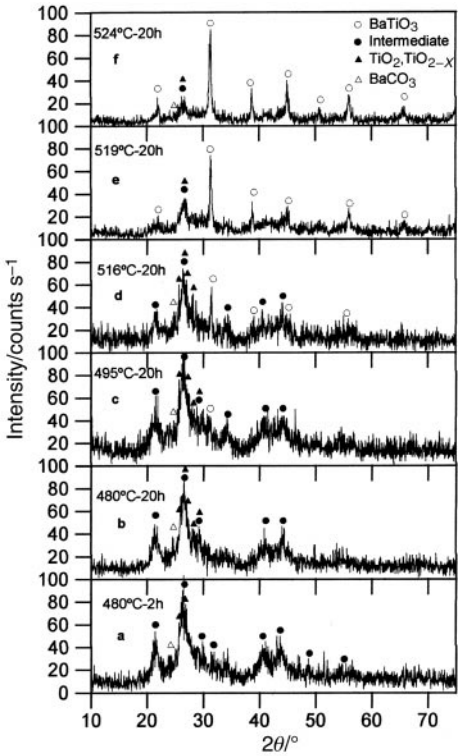

Fig. 11 Stability of the oxycarbonate intermediate phase with increasing temperature.

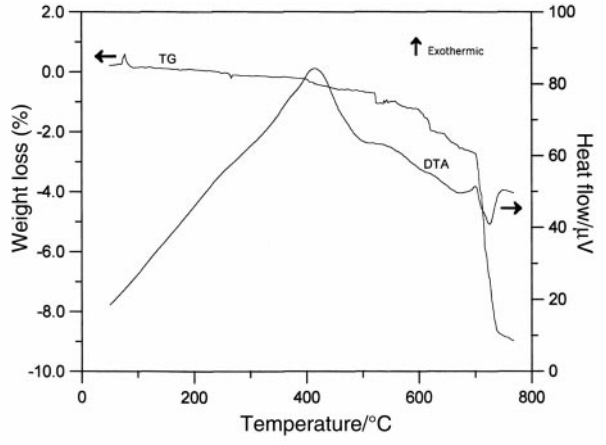

Fig. 12 TG and DTA of the oxycarbonate intermediate phase.

rate-controlling step of the $BaTiO_3$ formation. Given that the heating rate used for the synthesis of the oxycarbonate phase was relatively high, it can be suggested that such a phase was formed as a consequence of a transitory frozen non-equilibrium state in the beginning of an initial reaction between nanosized $BaCO_3$ and amorphous TiO_2, prior to the formation of the nanosized tetragonal and hexagonal $BaTiO_3$ polymorphs as the final products.

The TG/DTA curves, as shown in Fig. 12, recorded on the synthesised oxycarbonate intermediate phase show a wide exothermal effect between room temperature and about 690 °C, which can be attributed to the decomposition–oxidation of the organics, and a relatively small endothermic peak between 690 °C and about 750 °C which can be attributed to the thermal decomposition of the oxycarbonate intermediate phase. The weight loss between room temperature and about 690 °C was near 3%, and between 690 °C and 800 °C was about 6.2% which is slightly lower than that measured by Kumar *et al.*[9] for the thermal decomposition of this oxycarbonate phase (8.1%).

Fig. 13 compares the IR spectra recorded for this oxycarbonate phase with that of the PP powder at the same temperature. Two significant features are observed: (i) the appearance of two new peaks at 874 and 674 cm^{-1} which cannot be assigned to a barium oxide–titanium oxide system, and (ii) the IR bands at

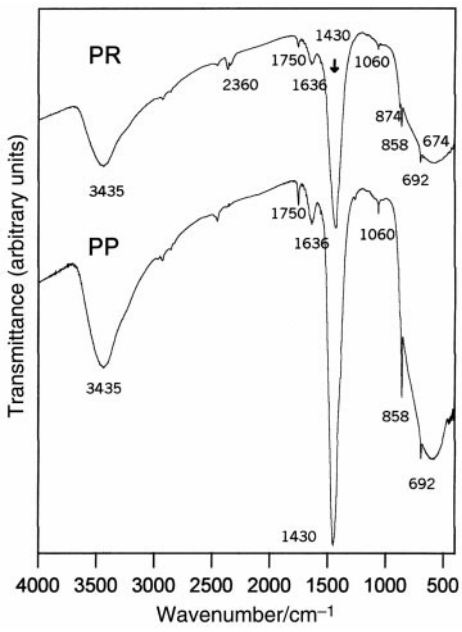

Fig. 13 FT-IR spectra of PR and PP powders heat-treated at 550 °C for 2 h showing the appearance of new IR features for the synthesized oxycarbonate intermediate phase.

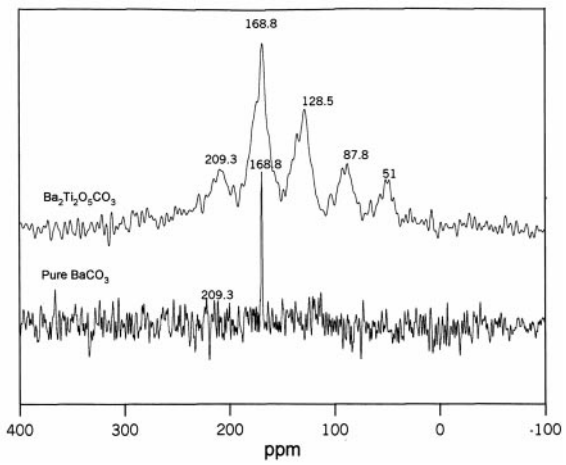

Fig. 14 ^{13}C NMR spectra for the synthesized oxycarbonate intermediate phase ($Ba_2Ti_2O_3$–CO_3) and pure $BaCO_3$.

1430, 1060, 858, and 692 cm^{-1}, characteristic of the CO_3^{2-} group, which are broader for this oxycarbonate intermediate phase. When comparing the Raman spectrum of this intermediate phase with that of the PP powder, a significant difference in the frequency of the characteristic peak for CO_3^{2-} ions (at about 1066 cm^{-1}, which is higher than that for pure $BaCO_3$ which is at about 1059 cm^{-1}), was also found.

Fig. 14 shows the solid-state ^{13}C NMR spectrum of the oxycarbonate intermediate phase, $Ba_2Ti_2O_5{\cdot}CO_3$, synthesized at 500 °C for 2 h. For comparison, the ^{13}C NMR spectrum of pure $BaCO_3$ is also shown. Several broad resonance signals appeared (chiefly those at 51, 87.8, 128.5, 168.8, and 209.3 ppm) which cannot be assigned to $BaCO_3$, with as is the case of the resonance absorptions at 168.8 and 209.3 ppm, the signals being much broader and with chemical shifts lower than those of $BaCO_3$. Therefore, even assuming comparable positions for these resonance peaks hypothetically attributable to $BaCO_3$, their broadened nature, together with the absence of $BaCO_3$ as suggested by the XRD measurement, see Fig. 10, suggests that the new ^{13}C NMR resonance signals should be assigned to the carbonate ions of the intermediate phase $Ba_2Ti_2O_5{\cdot}CO_3$ in close agreement with the results of Rajendran and Rao[25] and Tsay and Fang[22]

Discussion

The study of the thermal decomposition behavior of (Ba,Ti)-metal citrate polymerized resins in previous reports, was carried out by directly heating the polymerized resin at a predetermined heating rate in air.[8,9,21] Hennings and Mayr[8] and Arima *et al.*[21] assumed a molecular-level mixing of cations in the solution precursor, and that essentially the coordination of barium and titanium cations did not change on polymerization or even in the pyrolyzed resin at a temperature below 400 °C. On such a basis, the suggested reaction mechanisms for $BaTiO_3$ formation are very different. A solid-state reaction between nanosized $BaCO_3$ and amorphous TiO_2 was suggested by Hennings and Mayr,[8] and the formation of an oxycarbonate $Ba_2Ti_2O_5{\cdot}CO_3$ intermediate was concluded by Kumar *et al.*[9] and Arima *et al.*[21] More recently Tsay *et al.*[15,22] reported the formation of a metastable oxycarbonate intermediate phase with the structure of $BaTiO_3$ with carbonate ions located within the $BaTiO_3$ interlayers. On the other hand, no influence of the pH of the (Ba,Ti)-metal citrate solution precursor on the $BaTiO_3$ formation mechanism was also suggested, although the structure of the synthesized $BaTiO_3$ was not established.

Although the development of intermediate phases during the thermal decomposition of (Ba,Ti)–citrate polymerized precursors has been controversially disputed in the last ten years, no clearly distinguishable structural features for the so-called oxycarbonate intermediate phase, $Ba_2Ti_2O_5{\cdot}CO_3$, were reported. However, it is commonly accepted that such an intermediate phase is the key compound in the $BaTiO_3$ formation mechanism when polymerized organic precursors are used.[26] From the above experimental results, see Figs. 3–14, it is now well established that:

(i) the initial structure of the used precursor can influence the $BaTiO_3$ formation mechanism.

(ii) New structural features to distinguish the oxycarbonate intermediate phase are reported.

(iii) The structure of the formed $BaTiO_3$ is a mixture of hexagonal and tetragonal $BaTiO_3$ polymorphs and not the pseudo-cubic polymorph.

From Fig. 3 it can be clearly seen that the stretching modes at 1736 and 1569 cm^{-1} corresponding to ester and bridging complex, respectively, almost completely disappeared when the (Ba,Ti)–citrate gel was prepyrolyzed at 400 °C for 4 h. On the other hand, new weak but sharp peaks at 1450, 1059, 857 and 670 cm^{-1} began to be developed. These changes in the IR spectrum indicate that some alterations have taken place in the nature of bonding between the barium and titanium cations and the carboxylate groups. An evolution from the unidentate and bridging complexes to ionic bonds seems to have occurred after heat-treatment.[22] Furthermore, the appearance of an IR band at about 589 cm^{-1} related to the Ti–O stretching modes corroborates the above. All of these IR features allow us to conclude that the structure of the (Ba,Ti)-polymeric resin collapses after heating at 400 °C, leading to the creation of many active sites in the neighbourhood of the barium and titanium cations. In fact, when these powders were exposed to ambient air for several days, incipient formation of $BaCO_3$ was detected by XRD measurements. This finding is in agreement with the suggestions of Coutures *et al.*[16] who found a mixture of $BaCO_3$ and a graphitic phase in samples calcined at 375 °C for many hours. In the present case, the $BaCO_3$ intermediate phase dominates $BaTiO_3$ formation. However, direct heating of the polyester resin led to $BaTiO_3$ formation *via* an oxycarbonate, $Ba_2Ti_2O_5{\cdot}CO_3$, intermediate phase.

Tsay *et al.*[15] claimed that, for the first time, the oxycarbonate intermediate phase, $Ba_2Ti_2O_5{\cdot}CO_3$, had been unambiguously established from their XRD and IR experimental results. Some broadening in the IR bands at 1425, 1050, and 860 cm^{-1} related to the carbonate ions with respect to those of the pure $BaCO_3$, and the appearance of some broad peaks in the XRD data of samples calcined at 500 and 550 °C supported the above statement. From our XRD, IR, Raman, and ^{13}C NMR data, see Figs. 6–14, new structural features are contributing to a better knowledge of such an intermediate phase. For example, our oxycarbonate intermediate phase is better characterized not only by the XRD data showing a not well crystallized single-phase (without the presence of any residual $BaCO_3$), see Fig. 7, but also by the appearance of two extra peaks at 875 and 674 cm^{-1} in the IR spectrum of PR samples calcined at 500 and 550 °C for 2 h, along with the already mentioned broadening of the IR bands related to the carbonate ions in the samples, see Fig. 6. Besides this, our Raman experimental results, see Fig. 9, show new features which characterized our oxycarbonate intermediate phase. The shift of the peak related to the carbonate ions from 1059 cm^{-1} (typical for pure $BaCO_3$) towards higher frequencies, 1064 cm^{-1} in PR samples heat-treated at 500 °C, and to 1066 cm^{-1} in those PR samples heat-treated at 550 °C for 2 h, along with a strong increasing in intensity of the carbonate ions peak, confirm the distinguishing characteristics of such an oxycarbonate intermediate phase developed when the starting raw material used for the $BaTiO_3$ synthesis is a (Ba,Ti)–polyester resin. The presence of broad bands in the Raman spectrum of the sample calcined at 550 °C may be related to incipient $BaTiO_3$ or alternatively the suggestion of a $BaTiO_3$ with interlayered CO_3^{2-} groups as

the structure for the oxycarbonate $Ba_2Ti_2O_5{\cdot}CO_3$ intermediate phase.[22] Finally, the much broader resonance signals for the carbonate ions in the ^{13}C NMR spectrum for such an oxycarbonate phase, see Fig. 14, support such a structure.

Above 550 °C the XRD patterns showed considerable peak broadening associated with the nanosize particle sizes and, therefore, poor crystallinity of the $BaTiO_3$ powders. According to our results, see Fig. 8, no evidence for splitting appeared which can lead one to assume a pseudo-cubic structure for the formed $BaTiO_3$ at this thermal level, as reported elsewhere.[27] However, as was previously suggested,[10] the appearance of a peak at 304 cm^{-1} in the Raman spectra indicates a certain distortion of Ti–O bonds within the TiO_6 octahedra of $BaTiO_3$. This fact allowed us to assume that the nanosized $BaTiO_3$ powders do not have cubic symmetry. On the other hand, the presence of a Raman band at about 638 cm^{-1}, which increased in intensity with the calcination temperature can be considered as representative of scattering from $BaTiO_3$ with hexagonal structure,[23] which can be stabilized at low temperature by the high surface free energy of the nanosized $BaTiO_3$ powders. From all these results it can be advanced that the nanosized powders prepared by thermal decomposition of a (Ba,Ti)–citrate organic complex in air, consists of a mixture of tetragonal and hexagonal $BaTiO_3$ polymorphs rather than cubic. Such a viewpoint is contradictory to the widely accepted critical particle size theory for the stabilization of the cubic $BaTiO_3$ polymorph,[27–29] but it is in close agreement with similar results attained on submicronized $BaTiO_3$ powders prepared by hydrothermal and sol–gel synthesis methods.[30,31] In summary, it is suggested that the structure of the $BaTiO_3$ powders calcined in the temperature range 5500–750 °C has tetragonal 4*mm* symmetry at the local level, and cubic *m*3*m* symmetry upon averaging. This suggestion implies the assumption of some disorder in the crystal structure of the nanosized $BaTiO_3$ powders.

Conclusions

The thermal decomposition in air of (Ba,Ti)–citrate complex precursors has proven an efficient route for the preparation of nanosized agglomerated powders of stoichiometric $BaTiO_3$. It has been established that previous heat-treatments of such a complex precursor at 250 or 400 °C led to a polyesterified amorphous resin or to an amorphous powder with a locally broken precursor structure in which the nature of the barium cation–carboxylate group bonding is altered. Starting from these two kinds of raw materials we can advance the following suggestions: (1) $BaTiO_3$ synthesis above 550 °C takes place *via* the formation of an oxycarbonate intermediate phase, $Ba_2Ti_2O_5{\cdot}CO_3$, in the first case, and through the formation of nanocrystalline $BaCO_3$, as the main intermediate phase in the second one; (2) although not well crystallized, the oxycarbonate intermediate phase has been synthesized at the temperature range 500–550 °C. Weight loss measured from TGA, the XRD data, and the new IR and Raman structural features have identified distinguishable characteristics for such an oxycarbonate phase. Along with the unique XRD pattern, the appearance of new IR bands for the out-of-plane vibrations modes of the carbonate ions, the clear shift in the wavenumbers of the carbonate ions in the Raman spectra, and broadening in the ^{13}C NMR resonance signals, enable us to suggest that such an oxycarbonate phase has a formula close to $Ba_2Ti_2O_5{\cdot}CO_3$, in which the carbonate ions are different to those of pure $BaCO_3$, probably being located within the $BaTiO_3$ interlayers;[22] and (3) based on the XRD data, Raman spectra, and crystal size measurements, the $BaTiO_3$ powders as synthesized in the temperature range 550–750 °C consist of a mixture of tetragonal and hexagonal phases rather than cubic. Raman spectra of $BaTiO_3$ powders with a particle size as small as 15–20 nm showed evidence for asymmetry within the TiO_6 octahedra of the $BaTiO_3$ lattice. On the other hand, the presence of the high-temperature hexagonal $BaTiO_3$ polymorph at low temperature can be rationalized by the extremely high surface free energy of the nanosized particle that can stabilize such a phase.

Acknowledgements

This work has been supported by the Spanish CICYT Grant No. MAT 97-0694-C 02-01.

References

1 W. S. Clabaugh, E. M. Swiggard and R. Gilchrist, *J. Res. Natl. Bur. Stand. USA*, 1956, **56**, 289.
2 P. K. Gallagher and J. Thomson Jr, *J. Am. Ceram. Soc.*, 1965, **48**, 644.
3 M. P. Pechini, *U.S. Pat.*, No 3330697, July 11, 1967.
4 B. J. Mulder, *Am. Ceram. Soc. Bull.*, 1970, **49**, 90.
5 P. A. Lessing, *Am. Ceram. Soc. Bull.*, 1989, **68**, 1002.
6 S. G. Cho, P. F. Johnson and R. A. Condrate, *J. Mater. Sci.*, 1990, **25**, 4738.
7 H. S. Gopalakrishnamurthy, M. S. Rao and T. R. N. Kutty, *J. Inorg. Nucl. Chem.*, 1975, **37**, 891.
8 D. Hennings and W. Mayr, *J. Solid State Chem.*, 1978, **26**, 329.
9 S. Kumar, G. L. Messing and W. B. White, *J. Am. Ceram. Soc.*, 1993, **76**, 617.
10 P. Durán, F. Capel, J. Tartaj and C. Moure, *J. Mater. Res.*, 2001, **16**, 197.
11 S. Gablenz, H. P. Abicht, E. Pippel, O. Lichtenberger and J. Woltersdorf, *J. Eur. Ceram. Soc.*, 2000, **20**, 1053.
12 O. O. Vasyl'kiv, A. V. Ragulya and V. V. Skorodhod, *Powder Metall. Met. Ceram.*, 1997, **36**, 277.
13 W. S. Cho, *J. Phys. Chem. Solids*, 1998, **59**(5), 659.
14 B. D. Cullity, *Elements of X-Ray Diffraction*, 2nd edn., Addison-Wesley, Reading, MA, 1978.
15 J. D. Tsay, T. T. Fang, T. A. Gubiotti and J. Y. Ying, *J. Mater. Sci.*, 1998, **33**, 3721.
16 J. P. Coutures, P. Odier and C. Proust, *J. Mater. Sci.*, 1992, **27**, 1849.
17 G. Busca, V. Buscaglia, M. Leoni and P. Nanni, *Chem. Mater.*, 1994, **6**, 955.
18 K. Nakamoto, *Infrared and Raman Spectroscopy of Inorganic and Coordination Compounds,* 4th edn., Wiley Press, New York, 1986, p. 231.
19 M. Stokenhuber, H. Mayer and J. A. Lercher, *J. Am. Ceram. Soc.*, 1993, **76**, 1185.
20 E. Breitmaner and W. Voelter, *^{13}C-NMR Spectroscopy*, Verlag Chemie, New York, 1978.
21 M. Arima, M. Kakihana, Y. Nakamura, M. Yasima and M. Yoshimura, *J. Am. Ceram. Soc.*, 1996, **79**, 2847.
22 J. D. Tsay and T. T. Fang, *J. Am. Ceram. Soc.*, 1999, **82**, 1409.
23 N. G. Eror, T. M. Loher and B. C. Cornilsen, *Ferroelectrics*, 1980, **28**, 321.
24 J. Wang, J. Fang, S. C. Ng, L. M. Gan, C. H. Chew, X. Wang and Z. Shen, *J. Am. Ceram. Soc.*, 1999, **82**, 873.
25 M. Rajendran and M. S. Rao, *J. Solid State Chem.*, 1994, **113**, 239.
26 D. Hennings, G. Rosenstein and S. Schreinemacher, *J. Eur. Ceram. Soc.*, 1991, **8**, 107.
27 K. Uchino, E. Sadanaga and T. Irose, *J. Am. Ceram. Soc.*, 1989, **72**, 1555.
28 D. Hennings and S. Schreinemacher, *J. Eur. Ceram. Soc.*, 1992, **9**, 41.
29 B. D. Begg, E. R. Vance and J. Novotny, *J. Am. Ceram. Soc.*, 1994, **77**, 3186.
30 M. H. Frey and D. A. Payne, *Phys. Rev. B*, 1996, **54**(5), 3158.
31 I. J. Clark, T. Takeuchi, N. Ohtori and D. C. Sinclair, *J. Mater. Chem.*, 1999, **9**, 83.